Enhancing quantum entanglement and quantum teleportation for two-mode squeezed vacuum state by local quantum-optical catalysis

Xue-xiang Xu*
Department of Physics, Jiangxi Normal University, Nanchang 330022, China
(Received 20 March 2015; published 16 July 2015; corrected 17 July 2015)

I theoretically investigate how the entanglement properties of a two-mode squeezed vacuum state (TMSVS) can be enhanced by operating quantum-optical catalysis on each mode of the TMSVS. The quantum-optical catalysis is simply mixing one photon at the beam splitter and post-select the beam-splitter (BS) output based on detection of one photon, first proposed by Lvovsky and Mlynek [Phys. Rev. Lett. **88**, 250401 (2002)]. I find that there exists some enhancement in the entanglement properties (namely, entanglement entropy, second-order Einstein-Podolsky-Rosen correlation, and the fidelity of quantum teleportation) in certain parameter ranges spanned by the low transmissivities of the BSs and the small squeezing parameter of the input TMSVS.

DOI: 10.1103/PhysRevA.92.012318 PACS number(s): 03.67.Bg, 05.30.−d, 03.65.Wj, 42.50.Dv

I. INTRODUCTION

Entangled resources are useful in quantum information processing, such as quantum teleportation [1], metrology [2], and communications [3]. Two-mode squeezed vacuum state (TMSVS) is one of the most popular (if not the most) tools for quantum-enhanced optical interferometers or continuous variable (CV) quantum information processing as it is a Gaussian and entangled state [4–6]. However, theoretical investigations have shown that Gaussian entangled resources have some restrictions [7,8]. For example, entanglement distillation from two Gaussian entangled states is impossible by Gaussian local operations and classical communication [9,10]. Therefore, it is desirable to seek for non-Gaussian entangled resources and operations which can be more efficient in the quantum information processing. In recent years, some entanglement criteria beyond the Gaussian regime, including all orders of Einstein-Podolsky-Rosen (EPR) correlations, have been proposed [11,12]. Moreover, it has been shown that non-Gaussian two-mode entangled states provide the benefits of enhancing the entanglement [13–16].

Previously, the effect on the entanglement has been theoretically analyzed based on the merit of concrete protocol, such as the degree of entanglement, the EPR correlation, and the fidelity of teleportation [13,14]. In fact, it was shown that the performance of every protocol was improved, implying that the entanglement of a non-Gaussian state must be enhanced [12]. In recent years, many schemes of generating two-mode non-Gaussian entangled states have been proposed. Among these schemes, performing non-Gaussian operation on a two-mode Gaussian state is a possible approach to generate non-Gaussian entangled resources [17,18]. These typical non-Gaussian operations include the elementary operations (i.e., photon addition $a^\dagger, b^\dagger$ and subtraction a, b) and their sequential operations (e.g., $ab, a^\dagger b^\dagger$) [19,20] as well as their coherent superposition (e.g., $a^{\dagger 2} + b^{\dagger 2}$) [21]. Recently, in order to implement multiple photon addition and subtraction on both modes of the TMSVS, Navarrete-Benlloch *et al.* [15] demonstrate that the entanglement generally increases with the number of such operations. On the other hand, one can generate non-Gaussian entangled resources by means of a linear or nonlinear quantum-optical system [22–24]. The systems generally consist of beam splitting, phase shifting, squeezing, displacement, and various detection.

About two decades ago, the concept of "conditional measurement" was proposed by Dakna *et al.* [25] . They generate a Schrodinger-cat-like state by using a simple beam-splitter (BS) scheme for a conditional measurement. Following Dakna's idea of conditional measurement, many schemes have been proposed to prepare quantum states [26–28]. Among these works, the typical proposal is the quantum-optical catalysis, proposed by Lvovsky and Mlynek [29]. They generated a coherent superposition state $t|0\rangle + \alpha|1\rangle$ by conditional measurement on a BS. This state was generated in one of the BS output channels if a coherent state $|\alpha\rangle$ and a single-photon Fock state $|1\rangle$ are present in two input ports and a single photon is registered in the other BS output. They call this transformation as "quantum-optical catalysis" because the single photon itself remains unaffected but facilitates the conversion of the target ensemble. Recently, Bartley *et al.* [30] perform quantum-optical catalysis to generate multiphoton nonclassical states, which create a wide range of nonclassical phenomena. Since performing quantum-optical catalysis on a single-mode Gaussian state can enhance nonclassicality of the given state, one can ask whether it is possible to enhance entanglement of a two-mode Gaussian state via quantum-optical catalysis. This issue will be addressed here.

In this paper, I propose a scheme to generate a two-mode non-Gaussian entangled state. This state is generated by operating quantum-optical catalysis on each mode of a TMSVS. I investigate the entanglement properties (the degree of entanglement and EPR correlation) and the quantum teleportation fidelity for the state I produce. I show that when ideal quantum-optical catalysis is used, the input Gaussian state can be transformed into a non-Gaussian state with higher entanglement.

The paper is organized as follows. In Sec. II, I begin with the generation of a non-Gaussian two-mode entangled state by operating quantum-optical catalysis from a two-mode squeezed vacuum state (TMSVS) and derive its normalization factor (i.e., success probability), which is important to discussing quantum properties. In Sec. III, I investigate the entanglement properties (degree of entanglement and EPR correlation) of the non-Gaussian state and analyze the effect of the local

*Corresponding author: xuxuexiang@jxnu.edu.cn

quantum-optical catalysis. Then, I consider the non-Gaussian entangled state as an entangled resource to teleport a coherent state in Sec. IV. The main results are summarized in Sec. V.

II. TWO-MODE NON-GAUSSIAN ENTANGLED STATE BY LOCAL QUANTUM-OPTICAL CATALYSIS

In this section, I make a brief review of quantum-optical catalysis and apply it to prepare a two-mode non-Gaussian quantum state. The theoretical scheme is proposed and the success probability is derived.

A. Theoretical scheme

The basic idea on the quantum-optical catalysis was introduced in Ref. [29]. The conceptual schematic is shown in Fig. 1. If an input state ρ_{in} and a single-photon Fock state $|1\rangle$ are present in the two input ports of the BS and a single photon $|1\rangle$ is registered in one BS output port, then a catalyzed state ρ_c can be generated in the other BS output channel.

My scheme is depicted in Fig. 2. Theoretically, the input TMSVS $|\psi_0\rangle_{ab}$ is obtained by applying the unitary operator $S_2(r)$ on the two-mode vacuum $|0_a,0_b\rangle$, i.e.,

$$|\psi_0\rangle_{ab} = S_2(r)|0_a,0_b\rangle = \frac{1}{\cosh r}\exp(a^\dagger b^\dagger \tanh r)|0_a,0_b\rangle = \frac{1}{\cosh r}\sum_{n=0}^{\infty}\tanh^n r|n_a,n_b\rangle, \quad (1)$$

where $S_2(r) = \exp[r(a^\dagger b^\dagger - ab)]$ is the two-mode squeezed operator and the values of r determine the degree of squeezing. The larger r, the more the state is squeezed. In particular, when $r = 0$, $|\psi_0\rangle_{ab}$ reduces to $|0_a,0_b\rangle$. Enlightened by the idea of quantum-optical catalysis, I prepare a state from the TMSVS $|\psi_0\rangle_{ab}$ by operating quantum-optical catalysis on each mode. Then, the prepared state $|\psi_{\rm LQC}\rangle_{ab}$ is given by

$$|\psi_{\rm LQC}\rangle_{ab} = \frac{1}{\sqrt{p_{cd}}}\langle 1_d|\langle 1_c|B_2B_1S_2(r)|0_a,0_b\rangle|1_c\rangle|1_d\rangle, \quad (2)$$

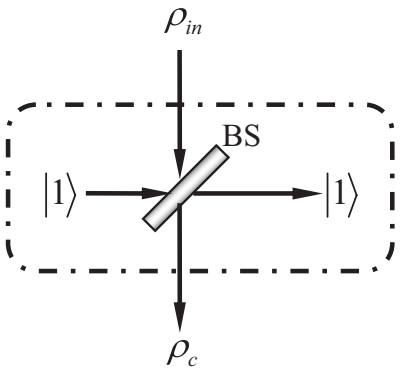

FIG. 1. Basic block of the quantum-optical catalysis. An input state ρ_{in} and a single-photon Fock state $|1\rangle$ are present in the two input ports of the BS. Measurement is conditioned on registering a single photon $|1\rangle$ by the single-photon detector. Here, the output state ρ_c is called as the catalysis state of the input state ρ_{in} and this process is quantum-optical catalysis. The catalysis parameter is the tunable transmissivity of the BS.

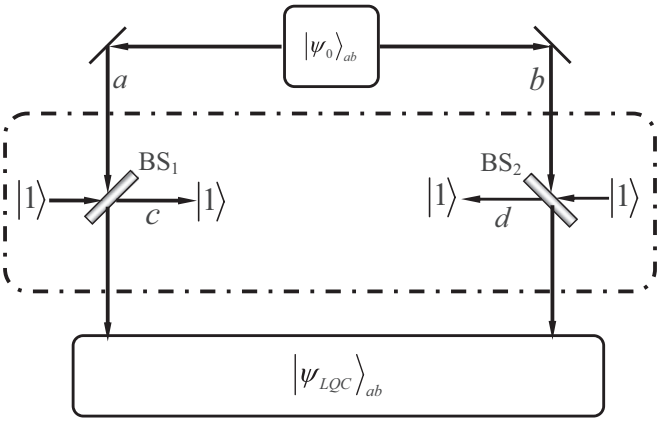

FIG. 2. Optical scheme to prepare a LQC-TMSVS by operating quantum-optical catalysis on each mode of a TMSVS. The input state is the TMSVS $|\psi_0\rangle_{ab}$ with the squeezing parameter r and the output state is the LQC-TMSVS $|\psi_{\rm LQC}\rangle_{ab}$ related with the input and catalysis parameter. The catalysis parameters are determined by the transmissivities T_1 and T_2 of the tunable BS_1 and BS_2, respectively. In contrast with the TMSVS, the LQC-TMSVS has a wide range of entanglement properties.

which will be called as "local quantum catalyzed TMSVS" (LQC-TMSVS). Here, B_1 and B_2 correspond to the respective unitary operators of the two tunable BS_1 and BS_2 with

$$B_1 = \exp[\theta_1(a^\dagger c - ac^\dagger)], \quad B_2 = \exp[\theta_2(b^\dagger d - bd^\dagger)] \quad (3)$$

in terms of the creation (annihilation) operator $a^\dagger$ (a), $b^\dagger$ (b), $c^\dagger$ (c), and $d^\dagger$ (d) for modes a, b, c, and d. Using Eq. (3), one obtains the following transformations:

$$\begin{aligned} B_1a^\dagger B_1^\dagger &= a^\dagger t_1 - c^\dagger r_1, \;\; B_1c^\dagger B_1^\dagger = a^\dagger r_1 + c^\dagger t_1, \\ B_2b^\dagger B_2^\dagger &= b^\dagger t_2 - d^\dagger r_2, \;\; B_2d^\dagger B_2^\dagger = b^\dagger r_2 + d^\dagger t_2, \end{aligned} \quad (4)$$

where $t_j = \cos\theta_j$ and $r_j = \sin\theta_j$ ($j = 1,2$) are the transmission coefficient and the reflection coefficient of the beam splitter BS_j, respectively. The normalization factor p_{cd} represents the success probability heralded by the detection of a single photon at the modes c and d.

Using the above relation and some technique (see Appendix A), the LQC-TMSVS $|\psi_{\rm LQC}\rangle_{ab}$ can be expressed explicitly as follows:

$$|\psi_{\rm LQC}\rangle_{ab} = (c_0 + c_1a^\dagger b^\dagger + c_2a^{\dagger 2}b^{\dagger 2})S_2(\lambda)|0_a,0_b\rangle, \quad (5)$$

where a squeezing parameter λ satisfying

$$\tanh\lambda = t_1t_2\tanh r,$$

and

$$c_0 = \frac{t_1t_2\cosh\lambda}{\sqrt{p_{cd}}\cosh r},$$

$$c_1 = \frac{\left(r_1^2r_2^2 - r_1^2t_2^2 - r_2^2t_1^2\right)\tanh r\cosh\lambda}{\sqrt{p_{cd}}\cosh r},$$

$$c_2 = \frac{r_1^2r_2^2\tanh r\sinh\lambda}{\sqrt{p_{cd}}\cosh r}.$$

Not surprisingly, the input TMSVS becomes non-Gaussian after the catalysis. From Eq. (5), I find that the LQC-TMSVS

$|\psi_{\rm LQC}\rangle_{ab}$ is actually a superposition state of $S_2(\lambda)|0_a,0_b\rangle$, $a^\dagger b^\dagger S_2(\lambda)|0_a,0_b\rangle$, and $a^{\dagger 2}b^{\dagger 2}S_2(\lambda)|0_a,0_b\rangle$ with a certain ratio. Note that the coefficients c_0, c_1, c_2, and λ are all the functions of the input squeezing parameter r and the transmission coefficients t_1,t_2 of the BSs. Meanwhile, this state can also be looked at as a non-Gaussian state by operating coherent superposition operator $(c_0 + c_1 a^\dagger b^\dagger + c_2 a^{\dagger 2} b^{\dagger 2})$ on $S_2(\lambda)|0_a,0_b\rangle$. So, I conclude that local quantum-optical catalysis operation plays a role of preparing the non-Gaussian entangled states. In the limit of $t_1 = t_2 = 1$, $|\psi_{\rm LQC}\rangle_{ab} \to |\psi_0\rangle_{ab}$, i.e., the output state is just the input one. While at least one of t_1,t_2 is zero, leading to $\lambda = 0$, $c_0 = 0$, $c_1 = 1$, $c_2 = 0$, so $|\psi_{\rm LQC}\rangle_{ab} \to |1_a,1_b\rangle$, i.e., the output state is a twin single-photon Fock state.

By the way, I often use the catalysis parameters $T_j = t_j^2$ $(j = 1,2)$ (i.e., the transmittance for each BS) in my following discussion and analysis. Compared with the input TMSVS, what optimal properties will emerge for the LQC-TMSVS? By tuning the input and catalysis parameters of the interaction, the LQC-TMSVS may be modulated, generating a wide range of entanglement phenomena, as I show in the next sections.

B. Success probability of detection

Normalization is important for discussing the properties of a quantum state. The normalization factor of the LQC-TMSVS in theory is actually the probability p_{cd} of detecting successfully single photon at the modes c and d in experiment. The density operator of the LQC-TMSVS $\rho_{\rm LQC} = |\psi_{\rm LQC}\rangle_{ab}\langle\psi_{\rm LQC}|$ is expressed in Appendix B. According to ${\rm Tr}(\rho_{\rm LQC}) = 1$, the success probability to get $|\psi_{\rm LQC}\rangle_{ab}$ from my proposal is given by

$$p_{cd} = p_0(a_0 + a_1\tanh^2 r + a_2\tanh^4 r + a_3\tanh^6 r + a_4\tanh^8 r), \quad (6)$$

with $p_0 = \cosh^{10}\lambda/\cosh^2 r$ and

$$\begin{aligned} a_0 &= t_1^2 t_2^2,\\ a_1 &= 1 - 4t_1^2 + 4t_1^4 - 4t_2^2 + 4t_2^4 + 16t_1^2t_2^2 - 16t_1^4t_2^2 - 16t_1^2t_2^4 + 11t_1^4t_2^4,\\ a_2 &= 11t_1^2t_2^2 - 28t_1^4t_2^2 - 28t_1^2t_2^4 + 64t_1^4t_2^4 + 16t_1^6t_2^2 + 16t_1^2t_2^6 - 28t_1^4t_2^6 - 28t_1^6t_2^4 + 11t_1^6t_2^6,\\ a_3 &= 11t_1^4t_2^4 - 16t_1^6t_2^4 - 16t_1^4t_2^6 + 4t_1^8t_2^4 + 4t_1^4t_2^8 + 16t_1^6t_2^6 - 4t_1^8t_2^6 - 4t_1^6t_2^8 + t_1^8t_2^8,\\ a_4 &= t_1^6t_2^6. \end{aligned}$$

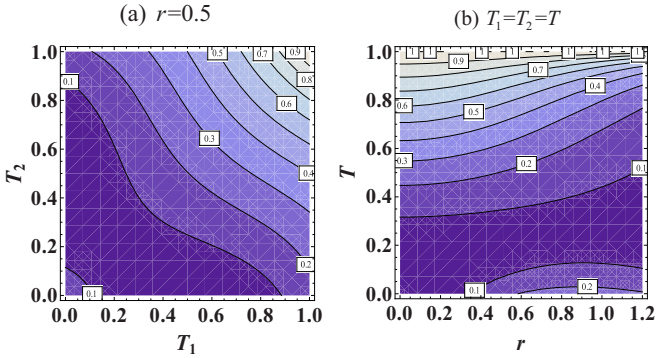

FIG. 3. (Color online) Success probability p_{cd} of detection as a function of the input parameter r and the catalysis parameter T_1, T_2 . (a) In (T_1,T_2) space for $r = 0.5$; (b) in (r,T) space.

In Fig. 3, I plot the distribution of the success probability p_{cd} in (T_1,T_2) space for $r = 0.5$ and in (r,T) space for the symmetric catalysis $T_1 = T_2 = T$. It is found that the detection probability of success is relatively low for the case of low transmissivity. The maximum success probability is 1 for the limit case of $T_1 = T_2 = 1$. While at least one of T_1,T_2 is zero, I find that $p_{cd} \to (1 - 2T_j)^2\tanh^2 r/\cosh^2 r$ $(j = 1,2)$.

III. ENTANGLEMENT PROPERTIES

In contrast with the input TMSVS, can the local quantum-optical catalysis be useful to enhance the entanglement properties? If possible, then how can I adjust the catalysis parameters in the process of preparing the LQC-TMSVS? In this section, I shall discuss the entanglement properties of the LQC-TMSVS quantified by the von Neumann entropy and the EPR correlation.

A. Degree of entanglement

Entanglement for a pure state in Schmidt form $|\psi\rangle_{ab} = \sum_n \omega_n|\alpha_n\rangle_a|\beta_n\rangle_b$ (ω_n real positive), with the orthonormal states $|\alpha_n\rangle_a$ and $|\beta_n\rangle_b$, is quantified by the partial von Neumann entropy of the reduced density operator, i.e.,

$$E(|\psi\rangle_{ab}) = -{\rm Tr}(\rho_a\log_2\rho_a) = -\sum_n \omega_n^2\log_2\omega_n^2, \quad (7)$$

where the local state is given by $\rho_a = {\rm Tr}_b(|\psi\rangle_{ab}\langle\psi|)$ [31]. The LQC-TMSVS $|\psi_{\rm LQC}\rangle_{ab}$ written in Schmidt form yields

$$|\psi_{\rm LQC}\rangle_{ab} = \sum_{n=0}^{\infty}\omega_n|n_a,n_b\rangle, \quad (8)$$

where the Schmidt coefficient is given by

$$\omega_n = \frac{(t_1^2 - n + nt_1^2)(t_2^2 - n + nt_2^2)(t_1t_2)^{n-1}\tanh^n r}{\sqrt{p_{cd}}\cosh r}. \quad (9)$$

The entanglement amount of the LQC-TMSVS $E(|\psi_{\rm LQC}\rangle_{ab})$ can be evaluated numerically by these Schmidt coefficients, as shown in Fig. 4.

In the limit cases, when at least one of t_1 or t_2 is zero, the output state corresponding to $|1_a,1_b\rangle$ is separate, $E = 0$. While $t_1 = t_2 = 1$, leading to $\omega_n^2 = \tanh^{2n} r/\cosh^2 r$, the output state is just the TMSVS (the input state), whose amount of entanglement is analytically given by [32,33]

$$E(|\psi_0\rangle_{ab}) = \cosh^2 r\log_2\cosh^2 r - \sinh^2 r\log_2\sinh^2 r. \quad (10)$$

In order to understand whether the entanglement is enhanced by local quantum-optical catalysis, I compare the von Neumann entropy values of the LQC-TMSVSs with the TMSVSs. If $E(|\psi_{\rm LQC}\rangle_{ab}) > E(|\psi_0\rangle_{ab})$, then the entanglement is enhanced in principle, or else it is weakened.

There are three feasibility regions having $E(|\psi_{\rm LQC}\rangle_{ab}) > E(|\psi_0\rangle_{ab})$, as shown in Fig. 5. One region is located in the low transmissivities of two BSs, i.e., $T_1,T_2 \in (0,0.5)$, the other two are located in one-small–one-large transmissivity of two

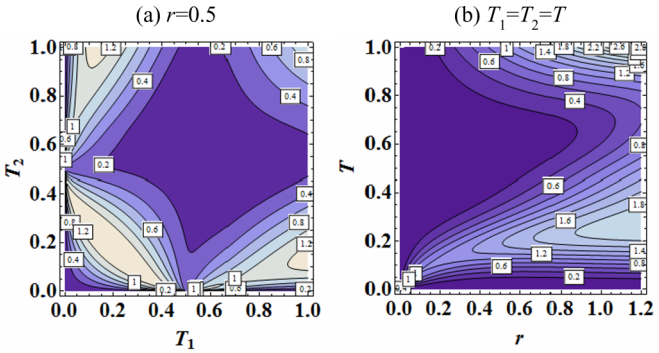

FIG. 4. (Color online) Neumann entropy E as a function of the input parameter r and the catalysis parameter T_1, T_2. (a) In (T_1, T_2) space for $r = 0.5$; (b) in (r, T) space.

BSs, i.e., $T_1 \in (0,0.5)$but $T_2 \in (0.5,1)$ or $T_2 \in (0,0.5)$but $T_1 \in (0.5,1)$. Three sections of Fig. 5 with $r = 0.02, 0.2, 0.7$ are reshaped in Fig. 6. With increasing the input parameter r, the enhancement region decreases and disappears at threshold $r = 0.785$, as shown in Fig. 6.

Next, I discuss the symmetric catalysis case, i.e., assuming $T = T_1 = T_2$. The feasibility region for enhancing the entanglement is depicted in the (r, T) plain space in Fig. 7. The enhancement happens in small-squeezing $(0 < r < 0.785)$ and low-transmissivity $(0 < T < 0.25)$ regimes. In Fig. 8(a), I plot the von Neumann entropy $E(|\psi_{\mathrm{LQC}}\rangle_{ab})$ as a function of the input squeezing parameter r for different $T = 0.1, 0.3$, compared with $T = 1$ (corresponding to the input TMSVS). With reference to the curve of the TMSVS, one sees that the enhancement is possible for $T = 0.1$ but not for $T = 0.3$. Compared with the corresponding TMSVSs (the red dashed line), I plot the von Neumann entropy $E(|\psi_{\mathrm{LQC}}\rangle_{ab})$ as a function of the catalysis parameter T for different input parameter $r = 0.2, 0.785, 0.9$ in Figs. 8(b)–8(d). For instance,

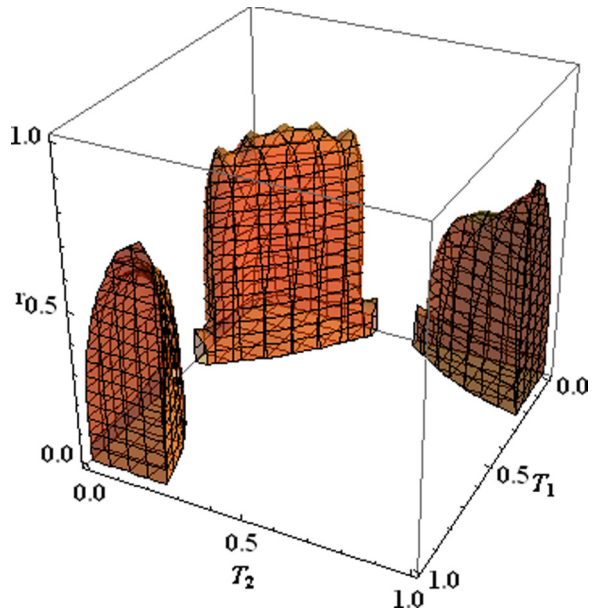

FIG. 5. (Color online) Three-dimensional plot of the feasibility region for $E(|\psi_{\mathrm{LQC}}\rangle_{ab}) > E(|\psi_0\rangle_{ab})$ in (r, T_1, T_2) space.

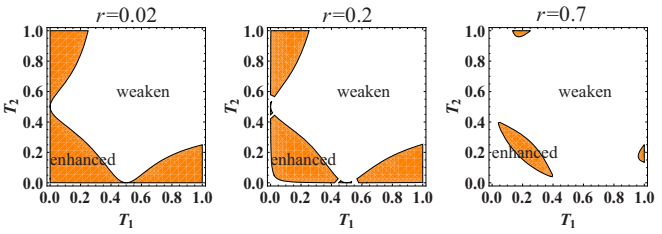

FIG. 6. (Color online) Plot of the feasibility region for $E(|\psi_{\mathrm{LQC}}\rangle_{ab}) > E(|\psi_0\rangle_{ab})$ in (T_1, T_2) space with different $r = 0.02, 0.2, 0.7$, also three sections of Fig. 5. If r is larger than a threshold value 0.785, the enhancement is impossible.

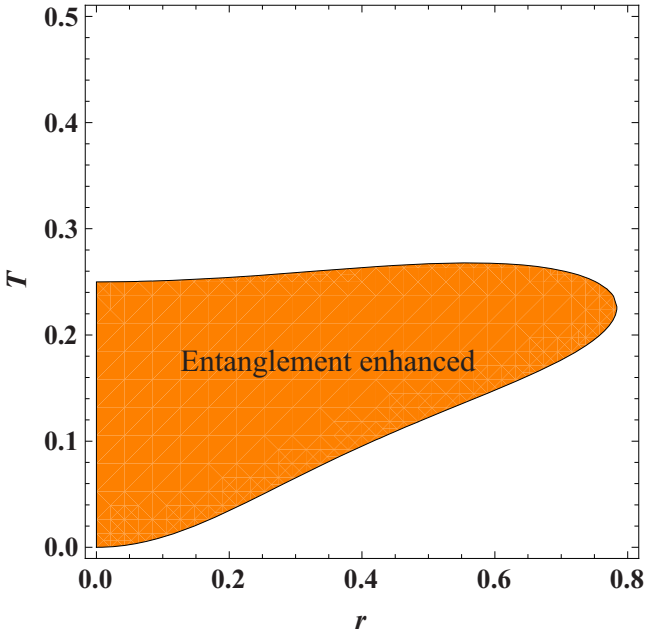

FIG. 7. (Color online) Plot of the feasibility region for enhancing entanglement, that is, $E(|\psi_{\mathrm{LQC}}\rangle_{ab}) > E(|\psi_0\rangle_{ab})$ in (r, T) space.

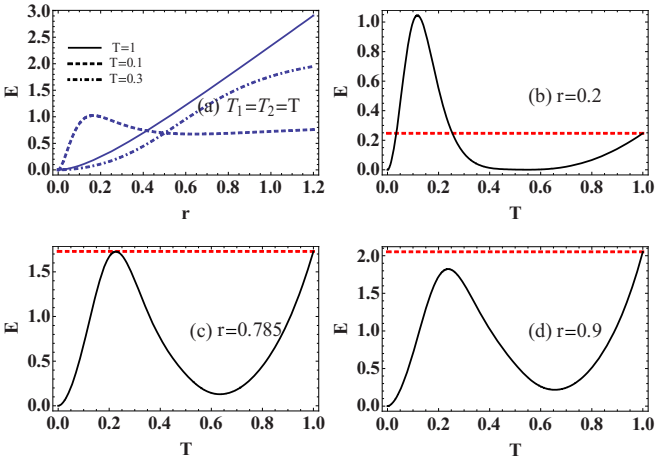

FIG. 8. (Color online) Neumann entropy $E(|\psi_{\mathrm{LQC}}\rangle_{ab})$ is depicted in (a) as a function of the input squeezing parameter r for different $T = 0.1, 0.3$, compared with $T = 1$ (corresponding to the input TMSVS); in (b)–(d) as a function of the catalysis parameter T (black solid line) for (b) $r = 0.2$, (c) $r = 0.785$, (d) $r = 0.9$, respectively, compared with their TMSVSs (red dashed line).

when $r = 0.2$, the enhancement of entanglement will happen in a certain catalysis range (about (0.03,0.23)) [see Fig. 8(b)]. But, above the threshold value $r = 0.785$, the enhancement is impossible, as shown in Fig. 8(d) for $r = 0.9$.

From the above discussion, I conclude that the degree of entanglement measured by the von Neumann entropy turns out to be enhanced only in the small-squeezing and low-transmissivity parameter spaces.

B. Second-order Einstein-Podolsky-Rosen correlation

For two-mode Gaussian entangled states, the entanglement can be fully described by the second-order Einstein-Podolsky-Rosen (EPR) correlation, which is characterized up to second-order moments of the state [34–36]. For two-mode non-Gaussian entangled states, however, the entanglement is fully described with all orders of moments [37,38]. It is known to all that a TMSVS (Gaussian) is the correlated state of two field modes a and b (signal and idle) that can be generated by a nonlinear medium [39]. But, after operating local quantum-optical catalysis on the TMSVS, how does the EPR correlation change? Here, I further investigate the EPR correlation, another entanglement property for the LQC-TMSVS.

The EPR correlation of two-mode states is the total variance of a pair of EPR-type operators

$$\begin{aligned} \mathrm{EPR} &= \Delta^2(x_a - x_b) + \Delta^2(p_a + p_b) \\ &= 2(1 + \langle a^\dagger a\rangle + \langle b^\dagger b\rangle - \langle a^\dagger b^\dagger\rangle - \langle ab\rangle) \\ &\quad - 2(\langle a\rangle - \langle b^\dagger\rangle)(\langle a^\dagger\rangle - \langle b\rangle), \end{aligned} \tag{11}$$

where $x_j = \frac{1}{\sqrt{2}}(j + j^\dagger)$ and $p_j = \frac{-i}{\sqrt{2}}(j - j^\dagger)$ $(j = a,b)$. For separable two-mode states or any classical two-mode states, the total variance is larger than or equal to 2 [34]. The condition EPR < 2, indicating quantum entanglement, can be an important resource in continuous variable quantum information processing protocols.

Given a LQC-TMSVS, one can evaluate the EPR correlation with the expectation values in Eq. (11). Using the general expression of $\langle a^{\dagger k_1} b^{\dagger k_2} a^{l_1} b^{l_2}\rangle$ in Appendix D, I prove that $\langle a^\dagger\rangle = \langle b^\dagger\rangle = \langle a\rangle = \langle b\rangle = 0$ and

$$\begin{aligned} \langle a^\dagger a\rangle &= M(x_0 + x_1 \tanh r + x_2 \tanh^2 r + x_3 \tanh^3 r \\ &\quad + x_4 \tanh^4 r + x_5 \tanh^5 r + x_6 \tanh^6 r \\ &\quad + x_7 \tanh^7 r + x_8 \tanh^8 r + x_9 \tanh^9 r), \end{aligned} \tag{12}$$

$$\begin{aligned} \langle b^\dagger b\rangle &= M(y_0 + y_1 \tanh r + y_2 \tanh^2 r + y_3 \tanh^3 r \\ &\quad + y_4 \tanh^4 r + y_5 \tanh^5 r + y_6 \tanh^6 r \\ &\quad + y_7 \tanh^7 r + y_8 \tanh^8 r + y_9 \tanh^9 r), \end{aligned} \tag{13}$$

as well as

$$\begin{aligned} \langle a^\dagger b^\dagger\rangle = \langle ab\rangle &= N(z_0 + z_1 \tanh r + z_2 \tanh^2 r \\ &\quad + z_3 \tanh^3 r + z_4 \tanh^4 r + z_5 \tanh^5 r \\ &\quad + z_6 \tanh^6 r + z_7 \tanh^7 r + z_8 \tanh^8 r), \end{aligned} \tag{14}$$

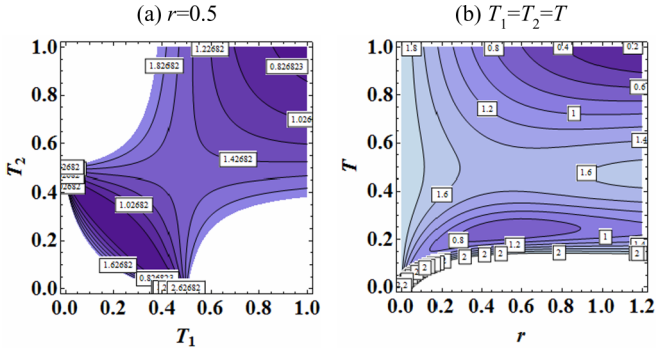

FIG. 9. (Color online) EPR correlation as a function of the input squeezing parameter r and the catalysis parameter T_1, T_2. (a) In (T_1, T_2) space for $r = 0.5$; (b) in (r, T) space. The colored region represents the condition EPR < 2.

where I have set x_i, y_i, z_i in Appendix E and

$$M = (\cosh^{12}\lambda \tanh r)/(p_{cd}\cosh^2 r),$$
$$N = (\cosh^{12}\lambda \tanh\lambda)/(p_{cd}\cosh^2 r).$$

Upon substituting the above equations into Eq. (11), the EPR correlation of the LQC-TMSVS $\mathrm{EPR}(|\psi_{\mathrm{LQC}}\rangle_{ab})$ can be calculated explicitly, which depends on the input squeezing degree r and the catalysis parameters T_1, T_2. In the limit of $T_1 = T_2 = 1$, $\mathrm{EPR}(|\psi_{\mathrm{LQC}}\rangle_{ab})$ reduces to $\mathrm{EPR}(|\psi_0\rangle_{ab}) = 2e^{-2r}$, which tends to zero asymptotically for $r \to \infty$. In Fig. 9, I plot the EPR correlation of the LQC-TMSVS in (T_1, T_2) space for $r = 0.5$ and in (r, T) space under the condition EPR < 2. One can see that there exists a threshold curve (boundary of EPR $= 2$) as a function of T_1 and T_2 for $r = 0.5$ in Fig. 9(a) and as a function of r and T in Fig. 9(b), respectively.

To exhibit whether the EPR correlation is enhanced, the fact that $\mathrm{EPR}(|\psi_{\mathrm{LQC}}\rangle_{ab})$ must be smaller than $\mathrm{EPR}(|\psi_0\rangle_{ab})$ must hold. The feasibility enhancement region of the EPR correlation is shown in Fig. 10. Three sections of Fig. 10 are shown in Fig. 11. Obviously, the enhancement happens only in one region with small squeezing and low transmissivity, unlike that of the degree of entanglement in Figs. 5 and 6. Moreover, with increasing the input parameter r, the enhancement region decreases and disappears at threshold $r = 0.585$.

The feasibility region for enhancing the EPR correlation is depicted in the (r, T) plain space in Fig. 12. For a small squeezing $(0 < r < 0.585)$ and low transmissivity $(0 < T < 0.3)$, the quantum-optical catalysis enhances the EPR correlation of the TMSVS (see Fig. 2). In Fig. 13, I plot the EPR correlation of the LQC-TMSVS as a function of r or T. In general, the EPR correlation of the TMSVS is enhanced with the squeezing parameter r, but it may not be always true for the case of $T = 0.1$, as shown in Fig. 13(a). I particulary compare the EPR correlation of the LQC-TMSVS with that of the TMSVS for the cases $r = 0.2, 0.585, 0.7$ in Figs. 13(b)–13(d). For a moderate catalysis parameter $0.12 < T < 0.3$, the catalysis operation gives the better EPR correlation for $r = 0.2$. For a large squeezing $(r > 0.585)$, the quantum-optical catalysis becomes the worse operation.

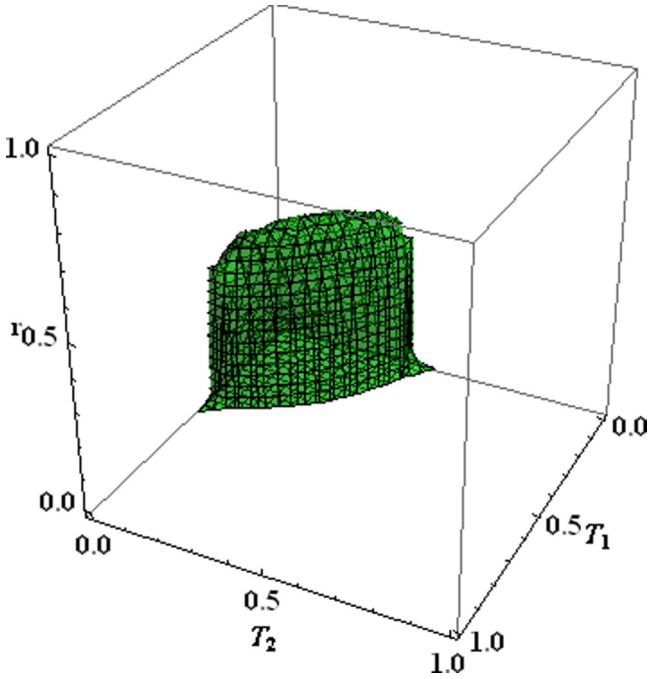

FIG. 10. (Color online) Three-dimensional plot of the feasibility region for enhancing EPR correlation, that is, $\mathrm{EPR}(|\psi_{\mathrm{LQC}}\rangle_{ab}) < \mathrm{EPR}(|\psi_0\rangle_{ab})$, in (r,T_1,T_2) space.

IV. QUANTUM TELEPORTATION USING NON-GAUSSIAN ENTANGLED STATE

After employing local quantum-optical catalysis on the TMSVS, I can see that the degree of entanglement and the EPR correlation can be enhanced in small-squeezing and low-transmissivity parameter regimes. Now, I consider the LQC-TMSVS as entangled resources in the Braunstein and Kimble (BK) protocol [1] to teleport a coherent state $|\gamma\rangle$ in CV teleportation. The fidelity between an input state and the output state is usually used as a measure to describe the quality of the quantum teleportation (QT).

For a CV system, a teleportation scheme has been proposed according to the characteristic functions (CFs) of the quantum states concluding input, source, and teleported states [40]. For the input coherent state, it is sufficient to calculate the teleportation fidelity for a particular input coherent state since there is no difference between the amplitudes of the input and

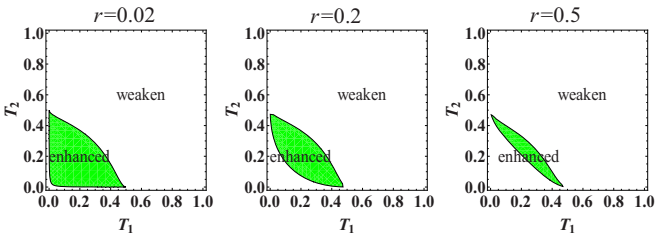

FIG. 11. (Color online) Plot of the feasibility region for enhancing EPR correlation, that is, $\mathrm{EPR}(|\psi_{\mathrm{LQC}}\rangle_{ab}) < \mathrm{EPR}(|\psi_0\rangle_{ab})$, in (T_1,T_2) space with different $r = 0.02,0.2,0.5$, also three sections of Fig. 10. If r is larger than a threshold value 0.585, the enhancement is impossible.

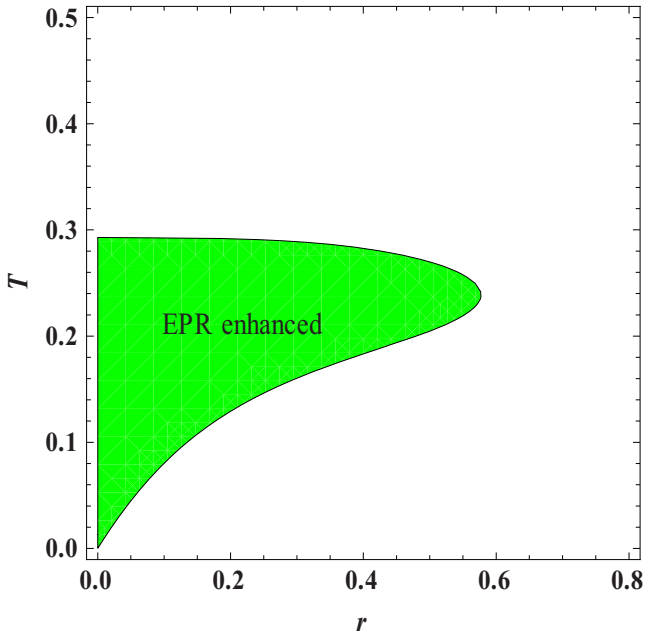

FIG. 12. (Color online) Plot of the feasibility region for enhancing EPR correlation, that is, $\mathrm{EPR}(|\psi_{\mathrm{LQC}}\rangle_{ab}) < \mathrm{EPR}(|\psi_0\rangle_{ab})$ in (r,T) space.

output coherent states in the BK protocol. For brevity, I take $\gamma = 0$, and then I only calculate the fidelity of teleporting the input vacuum state with the CF $\chi_{in}(z) = \exp[-|z|^2/2]$. The CF of the LQC-TMSVS (entangled resource or channel) $|\psi_{\mathrm{LQC}}\rangle_{ab}$ is given by

$$\chi_E(\alpha,\beta) = \mathrm{Tr}[D_a(\alpha)D_b(\beta)\rho_{\mathrm{LQC}}], \tag{15}$$

where $D_a(\alpha) = e^{\alpha a^\dagger - \alpha^* a}, D_b(\beta) = e^{\beta b^\dagger - \beta^* b}$ are the displacement operators. The detailed calculation procedure and result of $\chi_E(\alpha,\beta)$ are shown in Appendix F. The CF $\chi_{\mathrm{out}}(z)$ of the output state can be related to the CFs of the input state and the

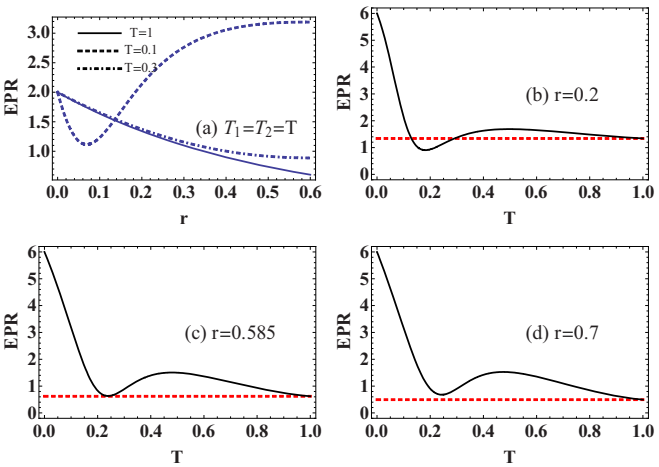

FIG. 13. (Color online) (a) EPR correlation as a function of the input parameter r for different $T = 0.1,0.3$, compared with $T = 1$ (corresponding to the input TMSVS); in (b)–(d) as a function of T for different input parameters $r = 0.2,0.585,0.7$, compared with their TMSVSs (the red dashed line).

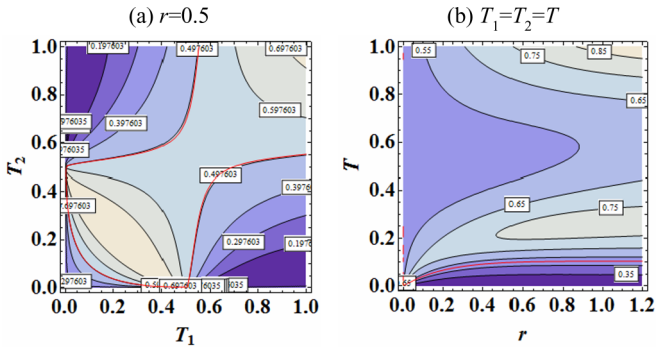

FIG. 14. (Color online) Teleportation fidelity of a coherent state with the LQC-TMSVS as a function of the input squeezing parameter r and the catalysis parameter T_1, T_2. (a) In (T_1, T_2) space for $r = 0.5$; (b) in (r, T) space. The red line is the boundary with $F = 0.5$.

entangled source by formula $\chi_{\rm out}(z) = \chi_{in}(z)\chi_E(z^*, z)$. Hence, the fidelity of QT of CVs can be obtained as [41]

$$F = \int \frac{d^2 z}{\pi} \chi_{in}(-z)\chi_{\rm out}(z). \tag{16}$$

Thus, F yields

$$F = \frac{p_0}{4p_{cd}}(m_0 + m_1 \tanh r + m_2 \tanh^2 r + m_3 \tanh^3 r + m_4 \tanh^4 r), \tag{17}$$

where

$$\begin{aligned} m_0 &= 2t_1^2 t_2^2, \\ m_1 &= 2t_1 t_2 - 4t_1^3 t_2 - 4t_1 t_2^3 - 2t_1^3 t_2^3, \\ m_2 &= 1 - 4t_1^2 + 4t_1^4 - 4t_2^2 + 4t_2^4 + 10t_1^2 t_2^2 \\ &\quad - 2t_1^4 t_2^2 - 2t_1^2 t_2^4 + 5t_1^4 t_2^4, \\ m_3 &= t_1 t_2 - t_1^3 t_2 - 2t_1^5 t_2 - t_1 t_2^3 - 2t_1 t_2^5 \\ &\quad - 2t_1^3 t_2^3 + t_1^5 t_2^3 + t_1^3 t_2^5 - 3t_1^5 t_2^5, \\ m_4 &= t_1^2 t_2^2 - t_1^4 t_2^2 + t_1^6 t_2^2 - t_1^2 t_2^4 + t_1^2 t_2^6 \\ &\quad + 2t_1^4 t_2^4 - t_1^6 t_2^4 - t_1^4 t_2^6 + t_1^6 t_2^6. \end{aligned}$$

In the limit case of $t_1^2 = t_2^2 = 1$, the fidelity of LQC-TMSVS $F(|\psi_{\rm LQC}\rangle_{ab})$ reduces to that of the TMSVS $F(|\psi_0\rangle_{ab}) = (1 + \tanh r)/2$, which is 0.5 for $r = 0$ and tends to 1 asymptotically for $r \to \infty$. In Fig. 14, I show the fidelity of teleporting a coherent state using the resource (LQC-TMSVS) in (T_1, T_2) space for $r = 0.5$ and in (r, T) space. The red line denotes the boundary with $F = 0.5$. The fidelity over the classical limit 0.5 may be considered as a successful quantum protocol [42].

Similar analysis of the teleportation fidelity is performed like that of the degree of entanglement and the EPR correlation in Sec. III. In Fig. 15, I plot the feasibility region for enhancing teleportation fidelity of a coherent state with the LQC-TMSVS, i.e., $F(|\psi_{\rm LQC}\rangle_{ab}) > F(|\psi_0\rangle_{ab})$, in (r, T_1, T_2) space. The figures in Fig. 16 are three sections of Fig. 15 with $r = 002, 0.2, 0.5$. In Fig. 17, I display the feasibility region in (r, T) space for enhancing teleportation fidelity of a coherent state using the LQC-TMSVS. The teleportation fidelity as a function of r or T is plotted in Fig. 18. Compared with the TMSVS as

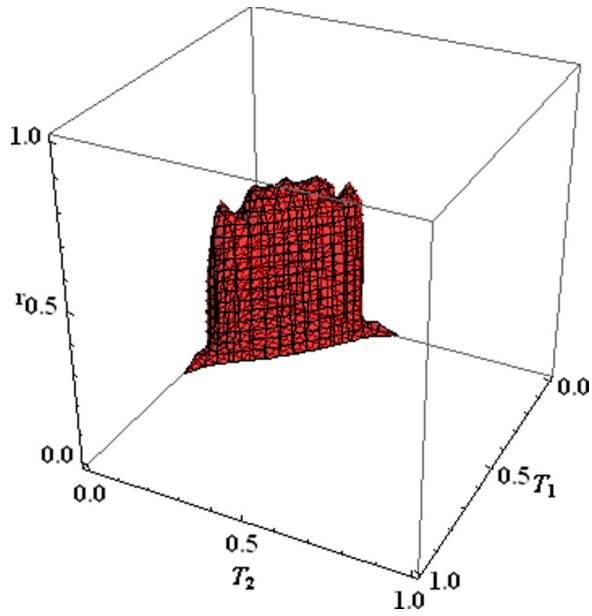

FIG. 15. (Color online) Three-dimensional plot of the feasibility region for enhancing teleportation fidelity of a coherent state with the LQC-TMSVS, that is, $F(|\psi_{\rm LQC}\rangle_{ab}) > F(|\psi_0\rangle_{ab})$, in (r, T_1, T_2) space.

the entangled resource, the enhancement of the teleportation fidelity is found in the range of $0 < r < 0.6$ and $0 < T < 0.27$. All these figures indicate that local quantum-optical catalysis can enhance the teleportation fidelity at the small-squeezing and low-transmissivity parameter regimes.

V. DISCUSSION AND CONCLUSION

Interestingly, when comparing the different enhancement feasibility regions of the quantities [degree of entanglement (orange), the EPR correlation (green), and the teleportation fidelity (red)] of the LQC-TMSVS in Figs. 5, 10, and 15 and 7, 12, and 17, I find that these enhancement regions do not overlap completely and locate in different input and catalysis parameter intervals. Taking the symmetric catalysis as example, the enhancement regions are different as (i) $0 < r < 0.785$ and $0 < T < 0.25$ for the degree of entanglement (ii) $0 < r < 0.585$ and $0 < T < 0.3$ for the EPR correlation; (iii) $0 < r < 0.6$ and $0 < T < 0.27$ for the teleportation fidelity. I further reshape each two of the three plots (Figs. 7, 12,

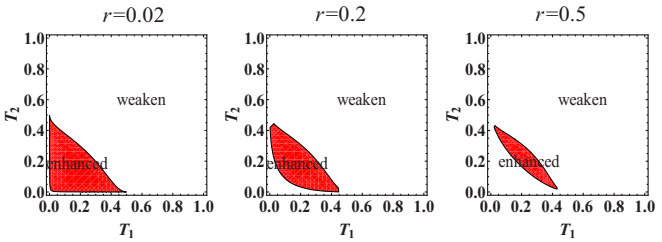

FIG. 16. (Color online) Plot of the feasibility region for enhancing teleportation fidelity of a coherent state with the LQC-TMSVS, that is $F(|\psi_{\rm LQC}\rangle_{ab}) > F(|\psi_0\rangle_{ab})$ in (T_1, T_2) space with different $r = 0.02, 0.2, 0.5$, also three sections of Fig. 15. If r is larger than a threshold value 0.6, the enhancement is impossible.

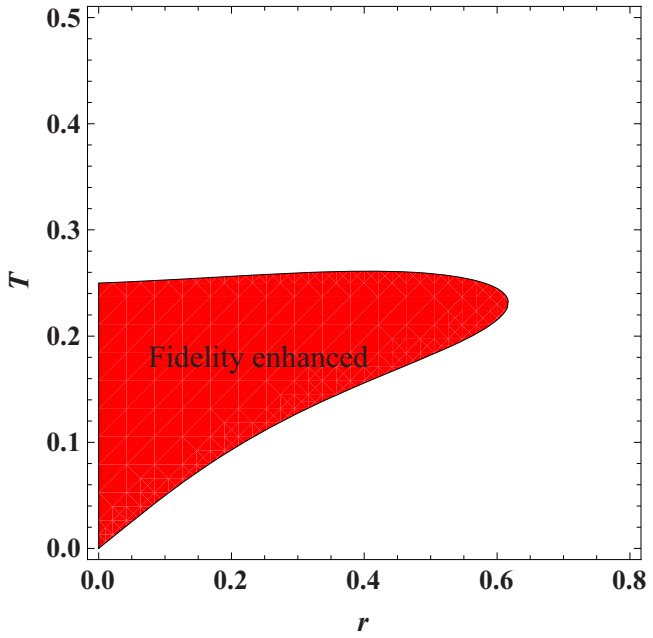

FIG. 17. (Color online) Plot of the feasibility region for enhancing teleportation fidelity of a coherent state with the LQC-TMSVS, that is, $F(|\psi_{\rm LQC}\rangle_{ab}) > F(|\psi_0\rangle_{ab})$ in (r,T) space.

and 17) in the same graph, as shown in Fig. 19. The conclusions are concluded by answering the following question: If A is enhanced, then must B be enhanced?, as demonstrated in Table I. For instance, there exists a parameter region where there is no EPR correlation enhancement, nevertheless, the fidelity enhancement is achieved [see the red area in Fig. 19(f)], so my answer is "no." For all these three quantities, there are common enhancement regions as shown in Fig. 20. This region locates in the regime of the relatively low beam-splitter transmissivities T_1 and T_2 (from 0 to around 0.25) and the

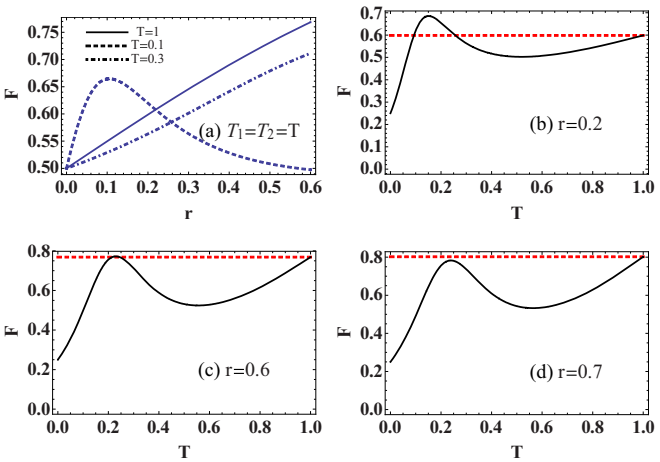

FIG. 18. (Color online) (a) Teleportation fidelity of a coherent state with the LQC-TMSVS as a function of the input parameter r for different $T = 0.1,0.3$, compared with $T = 1$ (corresponding to the input TMSVS); in (b)–(d) as a function of T for different input parameter $r = 0.2,0.6,0.7$, compared with their TMSVSs (the red dashed line).

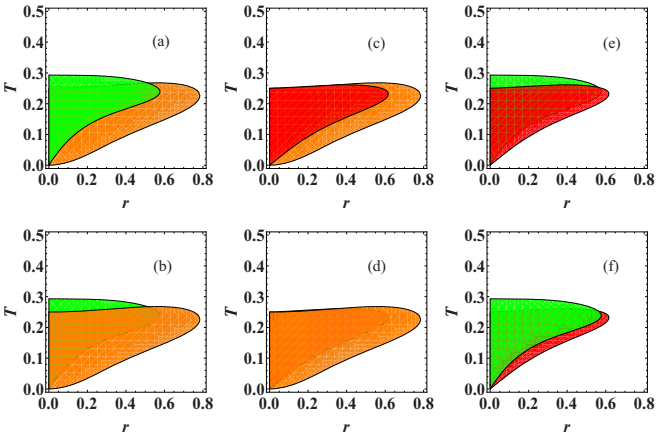

FIG. 19. (Color online) Comparison of the enhancing feasibility region for each two of the three properties, i.e., the degree of entanglement (orange, E), EPR correlation (green, EPR), and teleportation fidelity (red, F) in (r,T) space for symmetric catalysis. (a) E under EPR; (b) EPR under E; (c) E under F; (d) F under E; (e) EPR under F; (f) F under EPR. The stack-ups indicate the enhancement difference of these three properties. The illustration is explained in Table I.

small squeezing parameters (from 0 to around 0.6), which are the most experimentally accessible.

As the quantum-optical catalysis is an operation based on post-selection, the probability of success is naturally an issue. However, it is disadvantageous to see that the success probabilities in the most desirable parameter ranges (i.e., the enhancement regions) are relatively low in my protocol, as shown in Fig. 3. There is a fundamental tradeoff between success probability of the operation and the resultant enhancement in entanglement. In addition, the catalysis operation maximizes entanglement at low but nonzero probability. Thus, the success of detecting the single photon, also the key of the quantum-optical catalysis, is determined by the perfection of the detectors. As long as the detector is enough perfect, the single photon can be detected successfully. Using the current detection technology, the problem of low detection probability is possible to solve. This is good news. For example, the single photon can be counted by using superconducting single-photon detector with high efficiency (>90%), ultralow noise (<1 Hz), and low timing jitter (<100 ps) [43] . In experiment, it is possible to count near-infrared single photon with 95% efficiency. The measured 95% system detection efficiency is consistent with measurements and simulations of the optical elements [44] . On the other hand, the probability of success in

TABLE I. If A is enhanced, then must B be enhanced?

Case	A	B	Answer
Fig. 19(a)	E	EPR	No
Fig. 19(b)	EPR	E	No
Fig. 19(c)	E	F	No
Fig. 19(d)	F	E	Yes
Fig. 19(e)	EPR	F	No
Fig. 19(f)	F	EPR	No

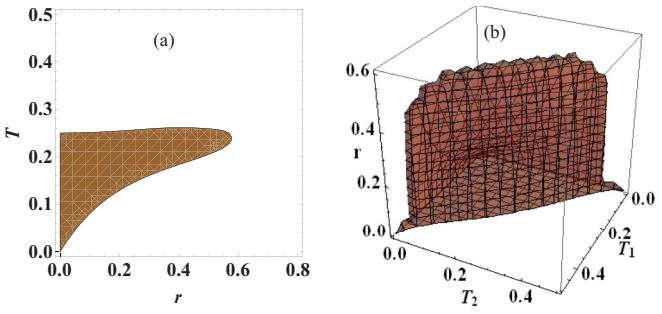

FIG. 20. (Color online) The common feasibility region for enhancing entanglement, EPR correlation, and teleportation fidelity in (r,T) space (a) and in (r,T_1,T_2) space (b). The brown regions are located at small-squeezing and low-transmissivity regimes.

experiment is actually the normalization factor for a prepared quantum state in theory. From the point of view of quantum mechanics, once the detection is succeeding, the quantum state can be generated.

In summary, this paper presents the effects of quantum optical catalysis on the two-mode squeezed vacuum in terms of various entanglement measures, namely, entanglement entropy, second-order EPR correlation, and the fidelity of quantum teleportation. The operation of the quantum-optical catalysis is a powerful tool which can be used to increase entanglement under certain conditions.

ACKNOWLEDGMENTS

The author would like to thank L.-y. Hu, Z.-s. Wang, Z.-l. Duan, J.-h. Huang, H.-c. Yuan, Q. Guo, and Y.-h. Li for helpful discussions. This work was supported by the National Nature Science Foundation of China (Grants No. 11264018 and No. 11447002) and the Natural Science Foundation of Jiangxi Province of China (Grants No. 20142BAB202001 and No. 20151BAB202013).

APPENDIX A: EXPLICIT FORM OF $|\psi_{\rm LQC}\rangle_{ab}$

In this appendix, I derive the the explicit form of $|\psi_{\rm LQC}\rangle_{ab}$. Noting the integral form of $|\psi_0\rangle_{ab}$,

$$|\Psi_0\rangle_{ab} = \frac{1}{\sinh r}\int \frac{d^2\alpha}{\pi} e^{-|\alpha|^2\tanh^{-1}r+\alpha a^\dagger+\alpha^* b^\dagger}|0,0\rangle$$

and the differential form of Fock state $|1\rangle$, such as $|1_c\rangle = \frac{d}{ds_1}e^{s_1c^\dagger}|0_c\rangle|_{s_1=0}$ and $|1_d\rangle = \frac{d}{ds_2}e^{s_2d^\dagger}|0_d\rangle|_{s_2=0}$, I rewrite $|\psi_{\rm LQC}\rangle_{ab}$ as

$$\begin{aligned}|\psi_{\rm LQC}\rangle_{ab} = {}& \frac{1}{\sqrt{p_{cd}}\sinh r}\frac{d^4}{ds_1ds_2ds_3ds_4}\int\frac{d^2\alpha}{\pi}e^{-|\alpha|^2\tanh^{-1}r}\\ &\times\langle 0_c|e^{s_3c}B_1e^{\alpha a^\dagger}e^{s_1c^\dagger}B_1^\dagger|0_a\rangle|0_c\rangle\\ &\times\langle 0_d|e^{s_4d}B_2e^{\alpha^* b^\dagger}e^{s_2d^\dagger}B_2^\dagger|0_b\rangle|0_d\rangle|_{(s_1,s_2,s_3,s_4)=0},\end{aligned}$$

where $(s_1,s_2,s_3,s_4)=0$ denotes $s_1=s_2=s_3=s_4=0$. Further using the transformation in Eq. (3), $B_1|0_a\rangle|0_c\rangle = |0_a\rangle|0_c\rangle$ and $B_2|0_b\rangle|0_d\rangle = |0_b\rangle|0_d\rangle$, I have

$$\begin{aligned}|\psi_{\rm LQC}\rangle_{ab} = {}& \frac{1}{\sqrt{p_{cd}}\sinh r}\frac{d^4}{ds_1ds_2ds_3ds_4}\int\frac{d^2\alpha}{\pi}e^{-|\alpha|^2\tanh^{-1}r}\\ &\times\langle 0_c|e^{s_3c}e^{c^\dagger(s_1t_1-\alpha r_1)}|0_c\rangle\langle 0_d|e^{s_4d}e^{d^\dagger(s_2t_2-\alpha^* r_2)}|0_d\rangle\\ &\times e^{a^\dagger(\alpha t_1+s_1r_1)}|0_a\rangle\otimes e^{b^\dagger(s_2r_2+\alpha^* t_2)}|0_b\rangle|_{(s_1,s_2,s_3,s_4)=0}.\end{aligned}$$

Inserting the completeness relation of coherent state $\int\frac{d^2z_j}{\pi}|z_j\rangle\langle z_j| = 1\ (j=1,2)$ in the appropriate place, I have

$$\begin{aligned}|\psi_{\rm LQC}\rangle_{ab} = {}& \frac{1}{\sqrt{p_{cd}}\sinh r}\frac{d^4}{ds_1ds_2ds_3ds_4}\int\frac{d^2\alpha}{\pi}e^{-|\alpha|^2\tanh^{-1}r}\\ &\times\langle 0_c|e^{s_3c}\int\frac{d^2z_1}{\pi}|z_1\rangle\langle z_1|e^{c^\dagger(s_1t_1-\alpha r_1)}|0_c\rangle\\ &\times\langle 0_d|e^{s_4d}\int\frac{d^2z_2}{\pi}|z_2\rangle\langle z_2|e^{d^\dagger(s_2t_2-\alpha^* r_2)}|0_d\rangle\\ &\times e^{a^\dagger(\alpha t_1+s_1r_1)+b^\dagger(s_2r_2+\alpha^* t_2)}|0_a,0_b\rangle|_{(s_1,s_2,s_3,s_4)=0}.\end{aligned}$$

After a straightforward integration, I finally arrive at the derivative form of $|\psi_{\rm LQC}\rangle_{ab}$:

$$\begin{aligned}|\psi_{\rm LQC}\rangle_{ab} = {}& \frac{1}{\sqrt{p_{cd}}\cosh r}\frac{d^4}{ds_1ds_2ds_3ds_4}\\ &\times e^{+s_3s_4r_1r_2\tanh r+s_1s_3t_1+s_2s_4t_2}\\ &\times e^{+a^\dagger s_1r_1-a^\dagger s_4t_1r_2\tanh r+b^\dagger s_2r_2-b^\dagger s_3t_2r_1\tanh r}\\ &\times e^{a^\dagger b^\dagger t_1t_2\tanh r}|0_a,0_b\rangle|_{(s_1,s_2,s_3,s_4)=0}.\end{aligned}$$

Therefore, the explicit form in Eq. (5) can be obtained after making derivation.

APPENDIX B: DENSITY OPERATOR $\rho_{\rm LQC} = |\psi_{\rm LQC}\rangle_{ab}\langle\psi_{\rm LQC}|$

The conjugate state of $|\psi_{\rm LQC}\rangle_{ab}$ can be given by

$$\begin{aligned}{}_{ab}\langle\psi_{\rm LQC}| = {}& \frac{1}{\sqrt{p_{cd}}\cosh r}\frac{d^4}{dh_1dh_2dh_3dh_4}\langle 0_a,0_b|e^{abt_1t_2\tanh r}\\ &\times e^{+ah_1r_1-ah_4t_1r_2\tanh r+bh_2r_2-bh_3t_2r_1\tanh r}\\ &\times e^{+h_3h_4r_1r_2\tanh r+h_1h_3t_1+h_2h_4t_2}|_{(h_1,h_2,h_3,h_4)=0}.\end{aligned}$$

Then, the density operator is

$$\begin{aligned}&\rho_{\rm LQC}\\ &= \frac{1}{p_{cd}\cosh^2 r}\frac{d^8}{ds_1ds_2ds_3ds_4dh_1dh_2dh_3dh_4}\\ &\times e^{+s_3s_4r_1r_2\tanh r+s_1s_3t_1+s_2s_4t_2}\\ &\times e^{+h_3h_4r_1r_2\tanh r+h_1h_3t_1+h_2h_4t_2}\\ &\times e^{a^\dagger s_1r_1-a^\dagger s_4t_1r_2\tanh r+b^\dagger s_2r_2-b^\dagger s_3t_2r_1\tanh r}\\ &\times e^{a^\dagger b^\dagger t_1t_2\tanh r}|0_a,0_b\rangle\langle 0_a,0_b|e^{abt_1t_2\tanh r}\\ &\times e^{ah_1r_1-ah_4t_1r_2\tanh r+bh_2r_2-bh_3t_2r_1\tanh r}|_{(s_1,s_2,s_3,s_4,h_1,h_2,h_3,h_4)=0}.\end{aligned}$$

APPENDIX C: SUCCESS PROBABILITY OF DETECTION

Due to $\mathrm{Tr}(\rho_{\mathrm{LQC}})=1$, I have

$$p_{cd}=\frac{\cosh^2\lambda}{\cosh^2 r}\frac{d^8}{ds_1ds_2ds_3ds_4dh_1dh_2dh_3dh_4}\times\exp(\Xi)|_{(s_1,s_2,s_3,s_4,h_1,h_2,h_3,h_4)=0},$$

where I have set

$$\begin{aligned}\Xi=&+\epsilon_1(s_3s_4+h_3h_4)+\epsilon_2(s_1s_2+h_1h_2)\\&+\epsilon_3(s_1s_3+h_1h_3)+\epsilon_4(s_2s_4+h_2h_4)\\&-\epsilon_5(h_2s_3+s_2h_3)-\epsilon_6(s_4h_1+s_1h_4)\\&+\epsilon_7s_1h_1+\epsilon_8s_2h_2+\epsilon_9s_3h_3+\epsilon_{10}s_4h_4\end{aligned}$$

with

$$\begin{aligned}&\epsilon_1=\frac{r_1r_2\sinh 2\lambda}{2t_1t_2},\quad \epsilon_2=\frac{r_1r_2\sinh 2\lambda}{2},\\&\epsilon_3=t_1\cosh^2\lambda-\frac{\sinh^2\lambda}{t_1},\\&\epsilon_4=t_2\cosh^2\lambda-\frac{\sinh^2\lambda}{t_2},\\&\epsilon_5=\frac{r_1r_2\sinh 2\lambda}{2t_1},\quad \epsilon_6=\frac{r_1r_2\sinh 2\lambda}{2t_2}\\&\epsilon_7=r_1^2\cosh^2\lambda,\quad \epsilon_8=r_2^2\cosh^2\lambda\\&\epsilon_9=\frac{r_1^2\sinh^2\lambda}{t_1^2},\quad \epsilon_{10}=\frac{r_2^2\sinh^2\lambda}{t_2^2}.\end{aligned}$$

APPENDIX D: EXPECTATION VALUE OF $\langle a^{\dagger k_1}b^{\dagger k_2}a^{l_1}b^{l_2}\rangle$

According to $\langle a^{\dagger k_1}b^{\dagger k_2}a^{l_1}b^{l_2}\rangle=\mathrm{Tr}(a^{\dagger k_1}b^{\dagger k_2}a^{l_1}b^{l_2}\rho_{\mathrm{LQC}})$ and making detailed calculation, I obtain

$$\begin{aligned}&\langle a^{\dagger k_1}b^{\dagger k_2}a^{l_1}b^{l_2}\rangle\\&=\frac{\cosh^2\lambda}{p_{cd}\cosh^2 r}\frac{d^{8+k_1+l_1+k_2+l_2}}{ds_1ds_2ds_3ds_4dh_1dh_2dh_3dh_4df_1^{k_1}df_2^{l_1}dg_1^{k_2}dg_2^{l_2}}\\&\times\exp(\Xi+\Theta)|_{(s_1,s_2,s_3,s_4,h_1,h_2,h_3,h_4,f_1,f_2,g_1,g_2)=0,}\end{aligned}$$

where I have set

$$\begin{aligned}\Theta=&+\eta_1(s_1g_1+h_1g_2)+\eta_2(s_2f_1+h_2f_2)\\&+\eta_3(s_2g_2+h_2g_1)+\eta_4(s_1f_2+h_1f_1)\\&-\eta_5(s_3g_2+h_3g_1)-\eta_6(s_4f_2+h_4f_1)\\&-\eta_7(s_4g_1+h_4g_2)-\eta_8(s_3f_1+h_3f_2)\\&+\eta_9(f_1g_1+f_2g_2)+\eta_{10}(f_1f_2+g_1g_2)\end{aligned}$$

with

$$\begin{aligned}&\eta_1=\frac{r_1\sinh 2\lambda}{2},\quad \eta_2=\frac{r_2\sinh 2\lambda}{2},\\&\eta_3=r_2\cosh^2\lambda,\quad \eta_4=r_1\cosh^2\lambda,\\&\eta_5=\frac{r_1\sinh 2\lambda}{2t_1},\quad \eta_6=\frac{r_2\sinh 2\lambda}{2t_2},\\&\eta_7=\frac{r_2\sinh^2\lambda}{t_2},\quad \eta_8=\frac{r_1\sinh^2\lambda}{t_1},\\&\eta_9=\frac{\sinh 2\lambda}{2},\quad \eta_{10}=\sinh^2\lambda.\end{aligned}$$

APPENDIX E: EXPRESSIONS OF x_i, y_i, z_i

Here, I list the expressions of x_i, y_i, and z_i as follows:

$$\begin{aligned}x_0=&-2t_1^2t_2^4+2t_1^4t_2^4,\\x_1=&1-4t_1^2+4t_1^4-4t_2^2+4t_2^4+16t_1^2t_2^2-16t_1^4t_2^2\\&-14t_1^2t_2^4+14t_1^4t_2^4+t_1^2t_2^6-2t_1^4t_2^6+t_1^6t_2^6,\\x_2=&4t_1^2t_2^2-12t_1^4t_2^2+8t_1^6t_2^2-16t_1^2t_2^4+48t_1^4t_2^4\\&-32t_1^6t_2^4+14t_1^2t_2^6-34t_1^4t_2^6+20t_1^6t_2^6,\\x_3=&22t_1^2t_2^2-60t_1^4t_2^2+40t_1^6t_2^2-56t_1^2t_2^4+146t_1^4t_2^4\\&-92t_1^6t_2^4+2t_1^8t_2^4+33t_1^2t_2^6-92t_1^4t_2^6+61t_1^6t_2^6\\&-8t_1^8t_2^6+4t_1^4t_2^8-8t_1^6t_2^8+4t_1^8t_2^8,\\x_4=&24t_1^4t_2^4-52t_1^6t_2^4+28t_1^8t_2^4-48t_1^4t_2^6+88t_1^6t_2^6\\&-40t_1^8t_2^6+20t_1^4t_2^8-34t_1^6t_2^8+14t_1^8t_2^8,\\x_5=&40t_1^4t_2^4-76t_1^6t_2^4+30t_1^8t_2^4-76t_1^4t_2^6+140t_1^6t_2^6\\&-56t_1^8t_2^6+4t_1^{10}t_2^6+36t_1^4t_2^8-58t_1^6t_2^8+26t_1^8t_2^8\\&-4t_1^{10}t_2^8+t_1^6t_2^{10}-2t_1^8t_2^{10}+t_1^{10}t_2^{10},\\x_6=&8t_1^6t_2^6-8t_1^8t_2^6-8t_1^6t_2^8+8t_1^8t_2^8+2t_1^6t_2^{10}-2t_1^8t_2^{10},\\x_7=&14t_1^6t_2^6-16t_1^8t_2^6+4t_1^{10}t_2^6-20t_1^6t_2^8+16t_1^8t_2^8\\&-4t_1^{10}t_2^8+5t_1^6t_2^{10}-4t_1^8t_2^{10}+t_1^{10}t_2^{10},\\x_8=&0,\quad x_9=t_1^8t_2^8,\end{aligned}$$

$$\begin{aligned}y_0=&-2t_1^4t_2^2+2t_1^4t_2^4,\\y_1=&1-4t_1^2+4t_1^4-4t_2^2+4t_2^4+16t_1^2t_2^2-16t_1^2t_2^4\\&-14t_1^4t_2^2+14t_1^4t_2^4+t_1^6t_2^2-2t_1^6t_2^4+t_1^6t_2^6,\\y_2=&4t_1^2t_2^2-16t_1^4t_2^2+14t_1^6t_2^2-12t_1^2t_2^4+48t_1^4t_2^4\\&-34t_1^6t_2^4+8t_1^2t_2^6-32t_1^4t_2^6+20t_1^6t_2^6,\\y_3=&22t_1^2t_2^2-56t_1^4t_2^2+33t_1^6t_2^2-60t_1^2t_2^4+146t_1^4t_2^4\\&-92t_1^6t_2^4+4t_1^8t_2^4+40t_1^2t_2^6-92t_1^4t_2^6+61t_1^6t_2^6\\&-8t_1^8t_2^6+2t_1^4t_2^8-8t_1^6t_2^8+4t_1^8t_2^8,\\y_4=&24t_1^4t_2^4-48t_1^6t_2^4+20t_1^8t_2^4-52t_1^4t_2^6+88t_1^6t_2^6\\&-34t_1^8t_2^6+28t_1^4t_2^8-40t_1^6t_2^8+14t_1^8t_2^8,\\y_5=&40t_1^4t_2^4-76t_1^6t_2^4+36t_1^8t_2^4-76t_1^4t_2^6+140t_1^6t_2^6\\&-58t_1^8t_2^6+t_1^{10}t_2^6+30t_1^4t_2^8-56t_1^6t_2^8+26t_1^8t_2^8\\&-2t_1^{10}t_2^8+4t_1^6t_2^{10}-4t_1^8t_2^{10}+t_1^{10}t_2^{10},\\y_6=&8t_1^6t_2^6-8t_1^8t_2^6-8t_1^6t_2^8+8t_1^8t_2^8+2t_1^{10}t_2^6-2t_1^{10}t_2^8,\end{aligned}$$

$$y_7 = 14t_1^6t_2^6 - 20t_1^8t_2^6 + 5t_1^{10}t_2^6 - 16t_1^6t_2^8 + 16t_1^8t_2^8 - 4t_1^{10}t_2^8 + 4t_1^6t_2^{10} - 4t_1^8t_2^{10} + t_1^{10}t_2^{10},$$

$$y_8 = 0, \quad y_9 = t_1^8t_2^8,$$

as well as

$$z_0 = 1 - 2t_1^2 - 2t_2^2 + 4t_1^2t_2^2,$$

$$z_1 = -t_1^2 + 2t_1^4 - t_2^2 + 2t_2^4 + 6t_1^2t_2^2 - 8t_1^4t_2^2 - 8t_1^2t_2^4 + 8t_1^4t_2^4,$$

$$z_2 = 8 - 27t_1^2 + 22t_1^4 - 27t_2^2 + 22t_2^4 + 87t_1^2t_2^2 - 67t_1^4t_2^2 + 2t_1^6t_2^2 - 67t_1^2t_2^4 + 49t_1^4t_2^4 - 6t_1^6t_2^4 + 2t_1^2t_2^6 - 6t_1^4t_2^6 + 4t_1^6t_2^6,$$

$$z_3 = 14t_1^2t_2^2 - 37t_1^4t_2^2 + 22t_1^6t_2^2 - 37t_1^2t_2^4 + 92t_1^4t_2^4 - 50t_1^6t_2^4 + 22t_1^2t_2^6 - 50t_1^4t_2^6 + 24t_1^6t_2^6,$$

$$z_4 = 45t_1^2t_2^2 - 98t_1^4t_2^2 + 48t_1^6t_2^2 - 98t_1^2t_2^4 + 197t_1^4t_2^4 - 90t_1^6t_2^4 + 4t_1^8t_2^4 + 48t_1^2t_2^6 - 90t_1^4t_2^6 + 46t_1^6t_2^6 - 6t_1^8t_2^6 + 4t_1^4t_2^8 - 6t_1^6t_2^8 + 2t_1^8t_2^8,$$

$$z_5 = 20t_1^4t_2^4 - 33t_1^6t_2^4 + 12t_1^8t_2^4 - 33t_1^4t_2^6 + 46t_1^6t_2^6 - 14t_1^8t_2^6 + 12t_1^4t_2^8 - 14t_1^6t_2^8 + 4t_1^8t_2^8,$$

$$z_6 = 24t_1^4t_2^4 - 31t_1^6t_2^4 + 8t_1^8t_2^4 - 31t_1^4t_2^6 + 33t_1^6t_2^6 - 9t_1^8t_2^6 + 8t_1^4t_2^8 - 9t_1^6t_2^8 + 3t_1^8t_2^8,$$

$$z_7 = 2t_1^6t_2^6 - t_1^8t_2^6 - t_1^6t_2^8, \quad z_8 = t_1^6t_2^6.$$

APPENDIX F: CHARACTERISTIC FUNCTION OF $|\Psi_{\rm LQC}\rangle_{ab}$

Noticing the displacement operators $D_a(\alpha) = e^{\frac{|\alpha|^2}{2}}e^{-\alpha^* a}e^{\alpha a^\dagger}, D_b(\beta) = e^{\frac{|\beta|^2}{2}}e^{-\beta^* b}e^{\beta b^\dagger}$, the CF of $|\psi_{\rm LQC}\rangle_{ab}$ can be calculated as

$$\chi_E(\alpha,\beta) = \frac{\cosh^2\lambda}{p_{cd}\cosh^2 r}\frac{d^8}{ds_1ds_2ds_3ds_4dh_1dh_2dh_3dh_4} \times e^{\Xi-\Lambda|\alpha|^2+\chi_\alpha\alpha+\chi_{\alpha^*}\alpha^*-\Lambda|\beta|^2+\chi_\beta\beta+\chi_{\beta^*}\beta^*+\eta_9(\alpha\beta+\alpha^*\beta^*)} \times|_{(s_1,s_2,s_3,s_4,h_1,h_2,h_3,h_4)=0},$$

where I have set $\Lambda = \cosh^2\lambda - \frac{1}{2}$ and

$$\chi_\alpha = h_1\eta_4 + s_2\eta_2 - s_3\eta_8 - h_4\eta_6,$$
$$\chi_{\alpha^*} = -s_1\eta_4 - h_2\eta_2 + h_3\eta_8 + s_4\eta_6,$$
$$\chi_\beta = s_1\eta_1 + h_2\eta_3 - h_3\eta_5 - s_4\eta_7,$$
$$\chi_{\beta^*} = -h_1\eta_1 - s_2\eta_3 + s_3\eta_5 + h_4\eta_7.$$

APPENDIX G: FIDELITY OF QT OF CVs

Considering the entangled state $|\psi_{\rm LQC}\rangle_{ab}$ to teleport a coherent (vacuum) state and substituting $\chi_{in}(z) = \exp[-|z|^2/2]$ and $\chi_{\rm out}(z) = \chi_{in}(z)\chi_E(z^*,z)$ into $F = \int\frac{d^2z}{\pi}\chi_{in}(-z)\chi_{\rm out}(z)$ yields

$$F = \frac{\kappa_0}{p_{cd}\cosh^2 r}\frac{d^8}{ds_1ds_2ds_3ds_4dh_1dh_2dh_3dh_4} \times \exp(\Pi)|_{(s_1,s_2,s_3,s_4,h_1,h_2,h_3,h_4)=0},$$

where I have set

$$\Pi = +\kappa_1(s_1s_2 + h_1h_2) + \kappa_2(s_3s_4 + h_3h_4) + \kappa_3(s_1s_3 + h_1h_3) + \kappa_4(s_2s_4 + h_2h_4) - \kappa_5(s_3h_2 + s_2h_3) - \kappa_6(s_4h_1 + s_1h_4) + \kappa_7s_1h_1 + \kappa_8s_2h_2 + \kappa_9s_3h_3 + \kappa_{10}s_4h_4$$

with $\kappa_0 = [2(1-\tanh\lambda)]^{-1}$ and

$$\kappa_1 = \kappa_0r_1r_2, \kappa_2 = \left(\kappa_0 + \frac{1}{2}\right)r_1r_2\tanh r,$$
$$\kappa_3 = \frac{t_1\sinh 2\lambda}{8\kappa_0} - \frac{\kappa_0\tanh\lambda}{t_1} + t_1\cosh^2\lambda,$$
$$\kappa_4 = \frac{t_2\sinh 2\lambda}{8\kappa_0} - \frac{\kappa_0\tanh\lambda}{t_2} + t_2\cosh^2\lambda$$
$$\kappa_5 = \frac{\kappa_0r_1r_2\tanh\lambda}{t_1}, \quad \kappa_6 = \frac{\kappa_0r_1r_2\tanh\lambda}{t_2},$$
$$\kappa_7 = \kappa_0r_1^2, \quad \kappa_8 = \kappa_0r_2^2,$$
$$\kappa_9 = \frac{\kappa_0r_1^2\tanh^2\lambda}{t_1^2}, \quad \kappa_{10} = \frac{\kappa_0r_2^2\tanh^2\lambda}{t_2^2}.$$

Thus, Eq. (17) can be obtained.

[1] S. L. Braunstein and H. J. Kimble, Phys. Rev. Lett. **80**, 869 (1998).
[2] P. M. Anisimov, G. M. Raterman, A. Chiruvelli, W. N. Plick, S. D. Huver, H. Lee, and J. P. Dowling, Phys. Rev. Lett. **104**, 103602 (2010).
[3] H. J. Briegel, W. Dur, J. I. Cirac, and P. Zoller, Phys. Rev. Lett. **81**, 5932 (1998).
[4] S. L. Braunstein and H. J. Kimble, Phys. Rev. A **61**, 042302 (2000).
[5] R. E. S. Polkinghorne and T. C. Ralph, Phys. Rev. Lett. **83**, 2095 (1999).
[6] P. van Loock and S. L. Braunstein, Phys. Rev. A **61**, 010302 (1999).
[7] S. D. Bartlett, B. C. Sanders, S. L. Braunstein, and K. Nemoto, Phys. Rev. Lett. **88**, 097904 (2002).
[8] S. D. Bartlett and B. C. Sanders, Phys. Rev. Lett. **89**, 207903 (2002).
[9] J. Eisert, S. Scheel, and M. B. Plenio, Phys. Rev. Lett. **89**, 137903 (2002).
[10] J. Fiurasek, Phys. Rev. Lett. **89**, 137904 (2002).
[11] H. Nha, S. Y. Lee, S. W. Ji, and M. S. Kim, Phys. Rev. Lett. **108**, 030503 (2012).

[12] A. Kitagawa, M. Takeoka, M. Sasaki, and A. Chefles, Phys. Rev. A **73**, 042310 (2006).
[13] S. Y. Lee, S. W. Ji, H. J. Kim, and H. Nha, Phys. Rev. A **84**, 012302 (2011).
[14] S. Y. Lee, S. W. Ji, and C. W. Lee, Phys. Rev. A **87**, 052321 (2013).
[15] C. Navarrete-Benlloch, R. Garcia-Patron, J. H. Shapiro, and N. J. Cerf, Phys. Rev. A **86**, 012328 (2012).
[16] Y. Yang and F. L. Li, Phys. Rev. A **80**, 022315 (2009).
[17] T. Opatrny, G. Kurizki, and D. G. Welsch, Phys. Rev. A **61**, 032302 (2000).
[18] P. T. Cochrane, T. C. Ralph, and G. J. Milburn, Phys. Rev. A **65**, 062306 (2002).
[19] F. D. Anno, S. D. Siena, and F. Illuminati, Phys. Rep. **428**, 53 (2006).
[20] M. S. Kim, J. Phys. B: At., Mol. Opt. Phys. **41**, 133001 (2008).
[21] S. Y. Lee and H. Nha, Phys. Rev. A **85**, 043816 (2012).
[22] J. Fiurasek, S. Massar, and N. J. Cerf, Phys. Rev. A **68**, 042325 (2003).
[23] H. Jeong, M. S. Kim, T. C. Ralph, and B. S. Ham, Phys. Rev. A **70**, 061801 (2004).
[24] E. Bimbard, N. Jain, A. MacRae, and A. I. Lvovsky, Nat. Photonics **4**, 243 (2010).
[25] M. Dakna, T. Anhut, T. Opatrny, L. Knoll, and D. G. Welsch, Phys. Rev. A **55**, 3184 (1997).
[26] M. Dakna, L. Knoll, and D. Welsch, Opt. Commun. **145**, 309 (1998).
[27] B. M. Escher, A. T. Avelar, and B. Baseia, Phys. Rev. A **72**, 045803 (2005).
[28] M. Takeoka and M. Sasaki, Phys. Rev. A **75**, 064302 (2007).
[29] A. I. Lvovsky and J. Mlynek, Phys. Rev. Lett. **88**, 250401 (2002).
[30] T. J. Bartley, G. Donati, J. B. Spring, X. M. Jin, M. Barbieri, A. Datta, B. J. Smith, and I. A. Walmsley, Phys. Rev. A **86**, 043820 (2012).
[31] C. H. Bennett, H. J. Bernstein, S. Popescu, and B. Schumacher, Phys. Rev. A **53**, 2046 (1996).
[32] S. J. van Enk, Phys. Rev. A **60**, 5095 (1999).
[33] J. Ryu, J. Lim, C. Lee, and J. Lee, J. Mod. Opt. **57**, 1550 (2010).
[34] L. M. Duan, G. Giedke, J. I. Cirac, and P. Zoller, Phys. Rev. Lett. **84**, 2722 (2000).
[35] R. Simon, Phys. Rev. Lett. **84**, 2726 (2000).
[36] G. Giedke, B. Kraus, M. Lewenstein, and J. I. Cirac, Phys. Rev. Lett. **87**, 167904 (2001).
[37] E. Shchukin and W. Vogel, Phys. Rev. Lett. **95**, 230502 (2005).
[38] M. Hillery and M. S. Zubairy, Phys. Rev. Lett. **96**, 050503 (2006).
[39] J. C. Garrison and R. Y. Chiao, *Quantum Optics* (Oxford University Press, New York, 2008).
[40] P. Marian and T. A. Marian, Phys. Rev. A **74**, 042306 (2006).
[41] A. V. Chizhov, L. Knoll, and D. G. Welsch, Phys. Rev. A **65**, 022310 (2002).
[42] S. L. Braunstein, C. A. Fuchs, H. J. Kimble, and P. van Loock, Phys. Rev. A **64**, 022321 (2001).
[43] F. Marsili, V. B. Verma, J. A. Stern, S. Harrington, A. E. Lita, T. Gerrits, I. Vayshenker, B. Baek, M. D. Shaw, R. P. Mirin, and S. W. Nam, Nat. Photonics **7**, 210 (2013).
[44] A. E. Lita, A. J. Miller, and S. W. Nam, Opt. Express **16**, 3032 (2008).